ELSEVIER

Journal of South American Earth Sciences 19 (2005) 415–432

Journal of
South American
Earth Sciences

www.elsevier.com/locate/jsames

# Geologic and tectonic setting of Deseado Massif epithermal deposits, Argentina, based on El Dorado-Monserrat

Leandro E. Echavarría[a,*], Isidoro B. Schalamuk[b], Ricardo O. Etcheverry[b]

[a]*Department of Geology and Geological Engineering, Colorado School of Mines, La Plata, Argentina*
[b]*CONICET-Instituto de Recursos Minerales, UNLP, Argentina, Facultad de Ciencias Naturales y Museo, UNLP, Avenida 122 y 60, La Plata 1900, Argentina*

Accepted 15 June 2005

**Abstract**

Middle–Late Jurassic bimodal volcanism, typical of a retroarc setting, developed during widespread extensional tectonism within the Deseado Massif, southern Argentina. This geologic environment led to the formation of numerous low-sulfidation epithermal deposits that are spatially and temporally related to the volcanic activity. The lack of significant high-sulfidation epithermal deposits may be because the tectonic and volcanic settings do not favor the formation of these types of deposits. El Dorado-Monserrat is a low-sulfidation epithermal prospect located near the southern boundary of the Deseado Massif. Mineralization is genetically linked to the Late Jurassic Chon Aike Formation and hosted by volcanic rocks of the middle Late Jurassic Bajo Pobre Formation. Two different mineralization areas have been identified. The Monserrat area is the most important, with veins hosted in a north-striking, left-lateral shear zone. The average thickness is 0.85 m, and the average metal content is 6.2 ppm gold and 153 ppm silver. The El Dorado area has discontinuous echelon veins within a right-lateral shear zone with low gold and silver grades. Hydrothermal alteration of the host rocks includes an inner zone of quartz-adularia and illite alteration and an outer zone of propylitic alteration. The main gangue mineral is quartz, which formed in successive pulses, plus adularia, pyrite, hematite, magnetite, and barite. Precious metals occur as zoned electrum. Ore mineral precipitation took place between 200 and 280 °C from low salinity fluids due to boiling.


**Resumen**

Un extenso volcanismo bimodal de ambiente de retroarco vinculado a una tectónica de extensión se desarrolló durante el Jurásico medio a superior en el Macizo del Deseado, sur de Argentina. En este ambiente geológico tuvo lugar la formación de numerosos depósitos epitermales de baja sulfuración, temporal y espacialmente relacionados a la actividad volcánica. La ausencia de depósitos epitermales de alta sulfuración de importancia sería el resultado del ambiente tectónico y volcánico que no favorecen el desarrollo de ese tipo de mineralización. El Dorado-Monserrat es un prospecto epitermal de baja sulfuración ubicado cerca del límite sudeste del Macizo del Deseado. La mineralización está genéticamente relacionada a la Formación Chon Aike del Jurásico superior y emplazada en andesitas correspondientes a la Formación Bajo Pobre, del Jurásico medio a superior. Se han reconocido dos áreas mineralizadas, el área de Monserrat es la de mayor importancia; allí, las vetas están emplazadas en una zona de cizalla sinestral de rumbo aproximado norte-sur. La potencia media de las vetas es de 0.85 m con un contenido de metales promedio de 6.2 ppm de oro y 153 ppm de plata. La zona de El Dorado, por su parte, presenta vetas discontinuas dispuestas en echelon dentro de una zona de cizalla de desplazamiento dextral con valores bajos en oro y plata. La alteración hidrotermal de las rocas de caja se caracteriza por un halo interno de alteración cuarzo-adularia e illita, que gradan a una zona externa de alteración propilítica. El mineral de ganga más abundante es cuarzo que ha sido depositado en pulsos sucesivos, acompañado por adularia, pirita, hematina, magnetita y baritina. El oro se encuentra como electrum que aparece con fuertes zonaciones. La precipitación de los minerales de mena y ganga tuvo lugar entre 200 y 280 °C a partir de fluidos diluidos. Se postula al proceso de ebullición como la causa principal que produjo la depositación mineral.


* Corresponding author.
*E-mail addresses:* inremi@infovia.com.ar (L.E. Echavarría), ischala@netverk.com.ar (I.B. Schalamuk).

0895-9811/$ - see front matter © 2005 Published by Elsevier Ltd.
doi:10.1016/j.jsames.2005.06.005

## 1. Introduction

The Deseado Massif is located in southern Patagonia, Argentina, and consists mainly of Middle–Late Jurassic silicic volcanic rocks that have been a target for precious metal exploration during the past 10 years, following the discovery of volcanic-hosted, epithermal gold and silver deposits. Discoveries include the Cerro Vanguardia, a world-class deposit of ~3.5 Moz gold equivalent; Manantial Espejo, the Martha mine, and the San José deposits; and prospects such as Josefina, El Dorado-Monserrat, La Manchuria, Bajo Pobre, Cerro Chato, and others (Fig. 1; Genini, 1988; Fernández and de Barrio, 1994; Del Blanco et al., 1994a; Schalamuk et al., 1994, 1995, 1997, 2002; Echavarría, 1995, 1997a; Echeveste et al., 1995; Zubia et al., 1999; Sanders, 2000). Most are good examples of Au-/Ag-rich, low-sulfidation vein systems hosted by Jurassic volcanic rocks, with only a few intermediate-sulfidation occurrences (i.e., Martha mine).

We first discuss the geologic environment of the Jurassic volcanism, including the stratigraphy, geochemistry, structural and geologic setting, and geochronology. We then present a structural, alteration, and mineralization case study for the El Dorado-Monserrat prospect based on geological mapping and mineralogical, textural, paragenetic, fluid inclusion, and stable isotope studies. The geological and metallogenic analysis presented herein provides new constraints on the characteristics of the precious metal epithermal mineralizations of the Deseado Massif.

El Dorado-Monserrat is an epithermal prospect located between 48°23′ and 48°26′S latitude and 68°34′ and 68°38′W longitude. The area is approximately 100 km northwest of Puerto San Julián and 20 km west of the Cerro Vanguardia mine. During the 1970s, minor barite was mined from one of the Monserrat veins, but an increasing amount of quartz intercalated with the barite led to its closure. What nobody knew until early 1990, when the San José and Minerales Patagonicos Mining companies mapped and sampled the veins in the area, was that the quartz was rich in gold and silver.

## 2. Regional geological setting

The Deseado Massif is located in the northeast Santa Cruz province, southern Argentina (Fig. 1). Isolated, small basement outcrops of low- to medium-grade metamorphic rocks belong to the Late Precambrian La Modesta Formation (Di Persia, 1960). Permian–Triassic sedimentary cover rocks were deposited in a rift basin during an initial extensional phase, followed by block faulting and the development of half-grabens containing lakes and deltas (Fig. 3; Homovc and Constantini, 2001). They consist of fluviolacustrine sandstone, siltstone, and conglomerate, evolving upward in the sequence to tuffaceous sandstone and laminated tuff.

During the Jurassic, intense extensional tectonism was accompanied by intermediate volcanism of the Bajo Pobre Formation, typified by fissure eruptions (Panza, 1995). In the Middle–Late Jurassic, there was an evolution toward more acidic volcanism that resulted in a large ignimbritic plateau of pyroclastic flows, laminated tuffs, lava flows, and megabreccias (de Barrio, 1993; Pankhurst et al., 1993). These rocks belong to the Chon Aike and La Matilde formations of the Bahía Laura Group. The extensional regime finished with the separation of the American and African continents and resulted in the opening of small basins that accumulated tuffaceous sediments of the Baqueró Formation during the Cretaceous (Archangelsky, 1967). Several marine incursions occurred since the Paleocene as the sea transgressed over the continental peneplain. Finally, during the Tertiary and Quaternary, olivine basalt flows and tuffs were deposited over large areas and today form erosionally dissected plateaus (Gorring et al., 1997; Panza and Franchi, 2002).

## 3. Middle–Late Jurassic volcanic province

### 3.1. Structural-tectonic setting

The tectonic evolution of the Deseado Massif during the Mesozoic is closely related to the breakup of Gondwana and the opening of the southern Atlantic Ocean (Uliana et al., 1989; Reimer et al., 1996; Ramos, 2002). During the Jurassic, the western margin of southern South America was actively subducting (Fig. 2; Nelson et al., 1980; Riccardi, 1983), and the backarc setting was undergoing broad extension. The extensional tectonism led to the formation of large, NNW-trending half-grabens, bounded by steeply dipping listric normal faults, most of which were reactivated structures of the former Permo-Triassic rift (Fig. 3; Gust et al., 1985; Uliana et al., 1989; Homovc and Constantini, 2001). Most of the half-grabens show the largest displacement on the west-dipping faults (Gust et al., 1985). Seismic and field evidence show that most of the Jurassic volcanism was deposited in the down-dropped blocks, resulting in thick volcanic sequences as thick as 2000 m, whereas there are only a few meters of an equivalent section present on the high side (Gust et al., 1985).

Extension took place simultaneously with the eruption of the Jurassic volcanic rocks and ended with the culmination of the volcanism or shortly thereafter. Paleogeographic reconstructions suggest an ENE-WSW propagation of the grabens during the Jurassic. The volcanotectonic province of the Deseado Massif during the Jurassic may be defined as a backarc extensional regime produced by either changes related to the subduction regime to the west (Gust et al., 1985) or emplacement of mantle plumes (Bruhn et al., 1978).

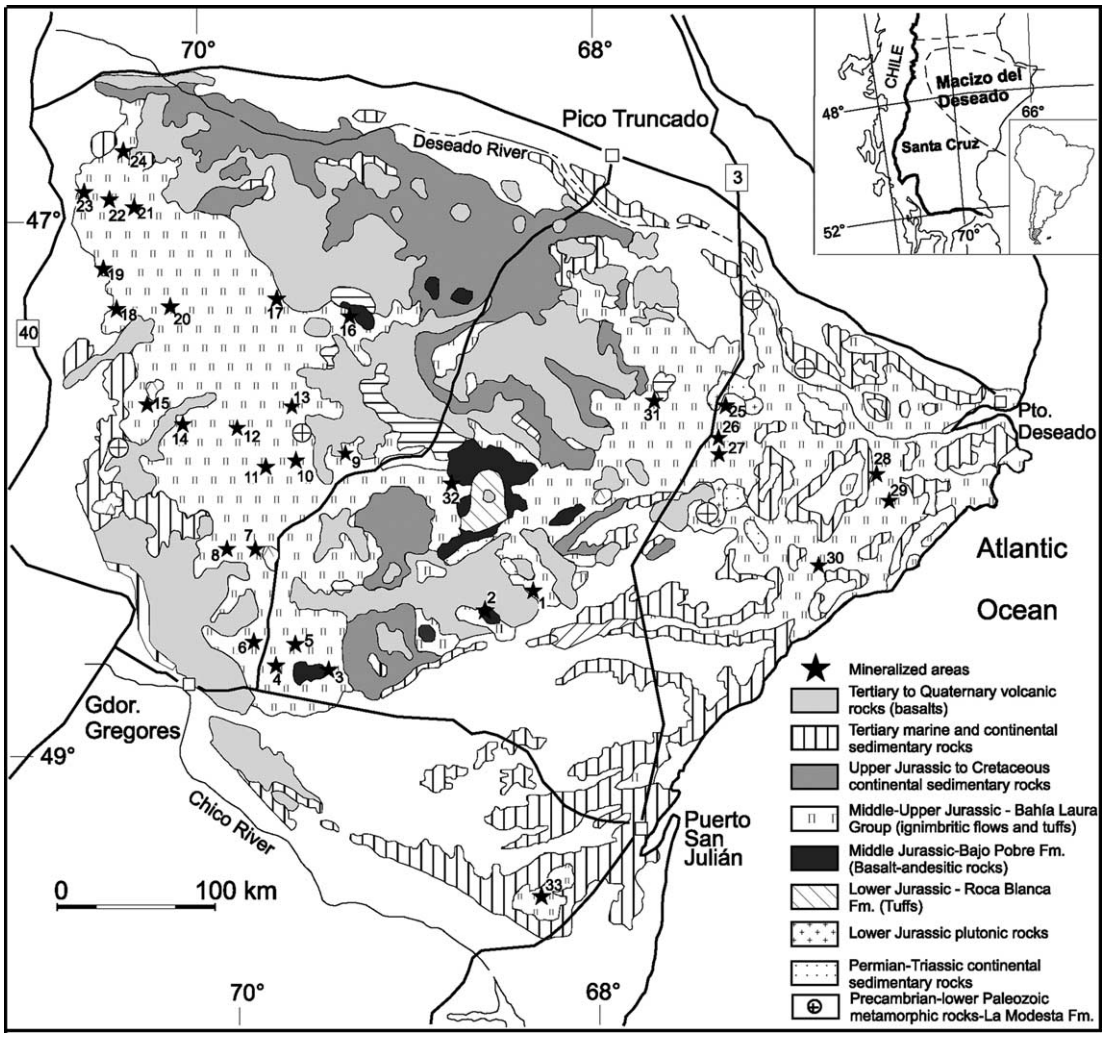


Fig. 1. Simplified geological map and location of major epithermal ore occurrences in the Deseado Massif, Argentina. Modified from Fernández and de Barrio (1994). Mineralized areas: (1) Cerro Vanguardia, (2) El Dorado-Monserrat, (3) Manantial Espejo, (4) Bacon (Martha mine), (5) La Rosita, (6) La Sarita, (7) La Manchuria, (8) Pilarica, (9) La Josefina, (10) La Valenciana, (11) Las Mellizas, (12) La Marcelina, (13) La Esperanza, (14) San Ignacio, (15) San Agustín, (16) Bajo Pobre, (17) El Macanudo, (18) El Cisne, (19) Río Pinturas, (20) Lejano, (21) Cerro Negro, (22) La Mariana-Eureka, (23) La Emilia, (24) San José, (25) Cerro Chato, (26) Martinetas, (27) Microondas, (28) Cerro Moro, (29) Bahía Laura, (30) Chispas, (31) La Paloma, (32) Piche, and (33) Laguna Guadalosa.

Shortly after emplacement of the volcanic province during the Early Cretaceous, there was a shift from extensional tectonics to transtensional and/or compressional tectonics (Reimer et al., 1996). However, during the Aptian, there was an extensional reactivation related to the eruption of a proximal facies of pyroclastics rocks of the Baquero Formation (Fig. 3; Ramos, 2002).

### 3.2. Stratigraphy

The Middle–Late Jurassic sequences comprise the Bajo Pobre, Chon Aike, and La Matilde formations, which cover approximately 100,000 km$^2$ in the Deseado Massif. Including the whole volcanic province of the now geographically separated formations in Patagonia and possibly west Antarctica, this area constitutes one of the most voluminous silicic volcanic provinces in the world, with a volume of ~235,000 km$^3$ (Pankhurst et al., 1998).

Although silicic rocks predominate, associated (and possibly cogenetic) mafic and intermediate rocks also are present. Mafic rocks are assigned to the Bajo Pobre Formation (Lesta and Ferello, 1972; De Giusto et al., 1980) and occur in extensive though discontinuous outcrops, with possible thicknesses of 200–600 m (De Giusto et al., 1980; Panza and Haller, 2002). The Bajo Pobre Formation consists of intermediate lava flows and tuffs. Lavas are aphanitic to finely porphyritic, with plagioclase and pyroxene phenocrysts. Clastic strata, including sandstones and conglomerates, are intercalated with the lavas. The upper part of the unit commonly consists of coarse volcanogenic conglomerates with basaltic to andesitic clasts. The intrusive facies consists of dikes and sills intruded in Triassic strata.

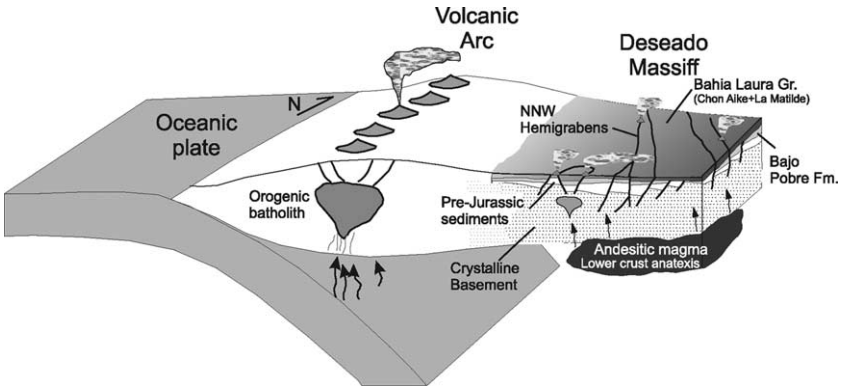


Fig. 2. Regional magmatic–tectonic model for the Deseado Massif during the Jurassic. Along the western margin of Gondwana, oceanic lithosphere was subducting beneath the continent. The backarc setting was subjected to extensional tectonics, developing NW-trending half-grabens. The effusion of volcanic rocks was related to the emplacement of magmas as the result of partial melting of the lower crust.

The Chon Aike and La Matilde formations comprise the Bahia Laura Group and form widespread outcrops throughout the Deseado Massif. The dominantly ignimbritic sequences are referred to the Chon Aike, whereas the interbedded, dominantly tuffaceous sequences are called La Matilde.

The Bahia Laura Group consists of volcanic and volcaniclastic rocks. Pyroclastic deposits, mainly ignimbrite, predominate with subordinate ash-fall tuffs and intercalated lava flows and domes. The ignimbrite comprises simple and complex cooling units, with individual units varying in thickness from a few centimeters to tens or 100 m (Pankhurst et al., 1998). The degree of welding is variable. In the Gran Bajo de San Julian district, poorly welded ignimbrites predominate (Sruoga and Irigoyen, 1987), whereas in the Cerro Vanguardia district, Sharpe et al. (2002) recognize intercalated, densely welded, and nonwelded ignimbrites. In the central part of the Deseado Massif, Echeveste et al. (2001) also describe densely welded (high-grade) ignimbrites intercalated with ash-fall tuffs. The welded ignimbrites are massive and commonly show columnar jointing; fiamme are abundant with high aspect ratios. The ignimbrites are either crystal or clast rich. The principal phenocrysts are quartz, K-feldspar, plagioclase, and biotite, and the accessories are magnetite, ilmenite, apatite, zircon, and monazite.

Rhyolitic domes and flows cut the pyroclastic sequence. They are porhyritic, quartz and K-feldspar rich, and flow banded and have autobreccias (Sruoga and Palma, 1986; Guido et al., 2002a,b; Echavarría, 1999).

The Jurassic volcanic rocks were subjected to low-grade regional metamorphism, hydrothermal alteration, and low-temperature hydration processes (Riley et al., 2001) that led to the formation of fine-grained quartz and K-feldspar aggregates, clays, illite, and silicification. Volcanic centers are not easily recognized within the Jurassic volcanic province of the Deseado Massif. Locally, small calderas are present (Fernández et al., 1996; Echavarría, 1999; Chernicoff and Salani, 2002), but they cannot explain the great volume of effusive rocks. Rather, it is believed that the eruptions of high-volume ignimbrites are fault-related fissure eruptions (e.g., Gust et al., 1985; Feraud et al., 1999), without the formation of prominent volcanic centers.

### 3.3. Geochemistry and petrogenesis

Major-element compositions within the whole Jurassic volcanic suite display strong bimodal distribution. The Bajo Pobre intermediate lavas have $SiO_2$ content of 51–63% (Fig. 4), whereas most of the Chon Aike pyroclastic rocks and lavas contain $>70\%$ $SiO_2$ (Fig. 4). Samples that plot between these groups are scarce (Fig. 4). The high-K silicic rocks of the Chon Aike formation are volumetrically much more important than the Bajo Pobre intermediate lavas. Major and rare earth element (REE) distribution show a typical calc-alkaline parentage (Fig. 5; Pankhurst and Rapela, 1995).

The $^{87}Sr/^{86}Sr$ initial ratios of Bajo Pobre rocks from the eastern Deseado Massif are indistinguishable from Chon Aike rocks, yielding an average of 0.7067 (Pankhurst and Rapela, 1995). However, Pankhurst et al. (1998) report slightly lower $(^{87}Sr/^{86}Sr)_i$ ratios (0.705–0.706) for the Bajo Pobre Formation in samples from the central portion of the Deseado Massif.

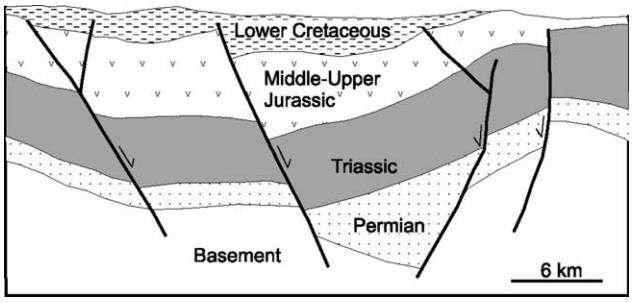


Fig. 3. Central Deseado Massif structure showing the configuration of the Permo-Triassic rift and its reactivation during the Middle–Late Jurassic and Early Cretaceous. Modified from Homovc and Constantini (2001).

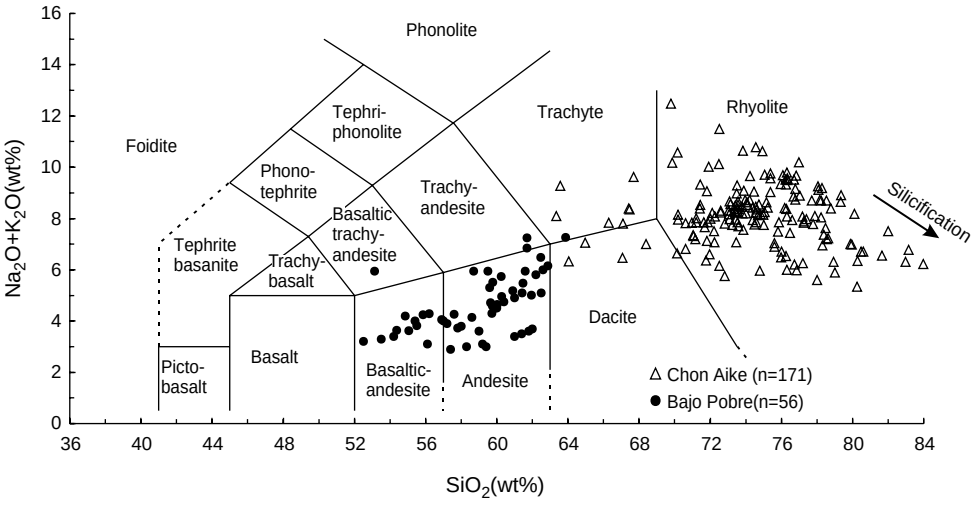


Fig. 4. Total alkali-silica diagram (Le Bas et al., 1986) for the Jurassic volcanic rocks (Bajo Pobre and Chon Aike formations) showing bimodal distribution. Extremely high silica content may reflect silicification due to postemplacement processes. Data from Gust et al. (1985), de Barrio (1989), Sruoga (1989), Pankhurst and Rapela (1995), Pankhurst et al. (1998), Echavarría (1999), Feraud et al. (1999), and the authors' unpublished data.

Postemplacement alteration is common in the Chon Aike Formation (Gust et al., 1985; Pankhurst et al., 1998; Riley et al., 2001), resulting in K- and Si-enrichment (Fig. 4) and a loss of Na. Such chemical mobility can result from hydrothermal alteration or low-grade metamorphism.

The geochemical signature of both silicic and intermediate rocks does not agree with mantle-derived sources; rather, the Jurassic volcanic rocks of the Deseado Massif appear to have been generated by partial fusion at the lower levels of the continental crust (Bruhn et al., 1978; Gust et al., 1985; Kay et al., 1989; de Barrio, 1993; Pankhurst and Rapela, 1995; Pankhurst et al., 1998). The heat necessary to produce partial fusion of the crust is thought to have come from the emplacement of voluminous mafic magmas at lower levels of the continental crust (Gust et al., 1985; Pankhurst et al., 1998).

### 3.4. Geochronology

Numerous geochronologic data of the Jurassic volcanic rocks of the Deseado Massif exist and are reviewed by Panza and Haller (2002). However, most geochronological work has been restricted to local areas without regional interpretation.

The intermediate volcanic rocks of the Bajo Pobre Formation show a high degree of alteration, making the acquisition of reliable geochronologic data difficult. However, several geochronological studies report high-precision Ar/Ar ages between 152.7±1.2 and 164.1±0.3 Ma (Alric et al., 1995, 1996; Feraud et al., 1999). Tessone et al. (1999) report an Rb/Sr isochron of 173±8 Ma. Taking into account these data, the Bajo Pobre Formation can be restricted to the Bathonian–Kimmeridgian (Middle–Late Jurassic).

Many geochronological studies have been made on the Chon Aike silicic volcanic rocks (e.g., Cazaneuve, 1965; Spalletti et al., 1982; de Barrio, 1993; Pankhurst et al., 1993; Alric et al., 1996; Arribas et al., 1996; Feraud et al., 1999; Tessone et al., 1999; Zubia et al., 1999). Chon Aike silicic volcanism is constrained between 177.8±0.8 and 148.8±3.6 Ma, which corresponds to a Bajocian–Tithonian age (Middle–Late Jurassic). Although the volcanic activity spanned more than 25 m.y., each eruption center was short lived, within 1–2 m.y. (Pankhurst and Rapela, 1995). Some authors (Pankhurst and Rapela, 1995; Alric et al., 1995; Feraud et al., 1999) have proposed that volcanic activity migrated from east to west and from north to south with time; however, Panza and Haller (2002) note that such

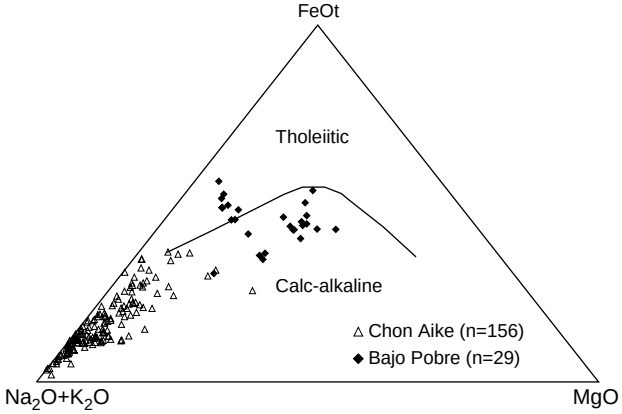


Fig. 5. AFM diagram for the Jurassic volcanic rocks (Bajo Pobre and Chon Aike formations) showing calc-alkaline trends. Tholeiitic and calc-alkaline fields from Irvine and Baragar (1971). Data from Gust et al. (1985), de Barrio (1989), Sruoga (1989), Pankhurst and Rapela (1995), Pankhurst et al. (1998), Echavarría (1999), Feraud et al. (1999), and the authors' unpublished data.

migration should be analyzed with caution due to the complexity of the sample location within the stratigraphic column of Jurassic volcanism and that more data are needed to constrain such an interpretation.

Rhyolites and andesites do not show systematic age differences, suggesting the contemporaneity of felsic and mafic volcanic activity at a given place (Feraud et al., 1999; de Barrio et al., 1999; Echeveste et al., 2001).

## 4. Deseado Massif epithermal deposits

The Middle–Late Jurassic volcanic rocks host numerous Au/Ag deposits and prospects (Fig. 1), leading Schalamuk et al. (1999a) to call the Deseado Massif a Au–Ag metallogenic province. Most of the reported occurrences correspond to the low-sulfidation epithermal category, as defined by Hedenquist et al. (2000). They are dominantly Au- and Ag-rich veins composed of multistage fracture fillings. Stockworks and disseminations occur but are not economically significant. The principal vein filling is silica, mainly as quartz and chalcedony, with minor barite and calcite and displays crustiform–colloform and recrystallization textures. Surface discharge of paleohydrothermal waters formed silica sinters in depressions that have been preserved from erosion in places, especially in the central and western part of the Deseado Massif, such as at La Josefina, La Marciana, and El Macanudo (Echeveste et al., 1995; Guido et al., 1999). The sinters are subhorizontal, approximately 3 m thick, and composed of laminated recrystallized quartz with bands that show slumping, mud cracks, nodular concentric textures, and reworked fragments.

Ore minerals, such as native gold, electrum, native silver, and argentite, occur disseminated in vein quartz and within weathering-derived goethite. The average grain size of gold and electrum is 10–50 μm. Other ore minerals described include tetrahedrite, galena, sphalerite, chalcopyrite, Ag sulfosalts, and Au tellurides, though always as minor components (Del Blanco et al., 1994b; Schalamuk et al., 1999a).

Geochronological data on epithermal adularia and illite from veins and hydrothermal alteration halos at different locations confirm the genetic relationship between Jurassic volcanism and the epithermal mineralization (Table 1). Arribas et al. (1996) report 10 K/Ar ages from hydrothermal illite at Cerro Vanguardia between 142.3 ± 3.4 and 152.4 ± 3.6 Ma. Dube et al. (2000) and Sharpe et al. (2002) present Ar–Ar dates on adularia from the Cerro Vanguardia Osvaldo Diez vein of 152.9 ± 2.75 to 157 ± 1.5 Ma. Other dates for the Manantial Espejo and Martinetas deposits also yield Upper Jurassic and even Lower Cretaceous ages (Table 1). For Manantial Espejo and Cerro Vanguardia deposits (Table 1), the age of the volcanic host rock is several million years older than that of the mineralization, which suggests that the hydrothermal systems were established during the latest, waning stages of volcanic activity.

The Deseado Massif epithermal veins were emplaced during a widespread extensional tectonic event, contemporaneous with the last stages of Chon Aike volcanism. The tension axis trended toward the NNE quadrant, producing left-lateral movement in fault and shear zones oriented between N10°E and N60°W and right-lateral movement in structures oriented between N30°E and N90°E. The former structures host the principle veins, which are continuous and thick, whereas the right-lateral structures develop only narrow, discontinuous, and *en echelon* veins of no economic significance.

Economic gold/silver mineralization is normally hosted in ore shoots, though at Cerro Vanguardia, Schalamuk et al. (1997) note a relatively homogeneous, atypical distribution; however, bonanza-type ore shoots extend along-strike, from 200 to 1200 m in length and vertically from 40 to 160 m (Schalamuk et al., 1997; Zubia et al., 1999). At the Martha mine, high-grade silver ore is located in an ore shoot that extends for approximately 200 m along-strike and 60 m vertically (Fig. 6). Formation of ore shoots is related to structural openings within regional shear zones. The Martha mine silver shoot is a good example of a dilational bend that

Table 1
Geochronological data for several Deseado Massif epithermal mineralized rocks

| Locality | Unit | Mineral | Method | Age | Reference |
|---|---|---|---|---|---|
| Co. Vanguardia | Hydrothermal Alt. Vanguardia vein | Illite | K/Ar | 149.5 ± 3.5, 152.4 ± 3.6 | Arribas et al. (1996) |
| Co. Vanguardia | Hydrothermal Alt. Osvaldo Diez vein | Illite | K/Ar | 142.3 ± 3.4, 151.0 ± 3.5 | Arribas et al. (1996) |
| Co. Vanguardia | Natalia vein | Adularia | K/Ar | 138.5 ± 3.3 | Arribas et al. (1996) |
| Co. Vanguardia | Osvaldo Diez vein | Adularia | | 157 ± 1.5 | Dube et al. (2000) |
| Co. Vanguardia | Chon Aike Fm. | Zircon? | U/Pb | 171.9 ± 1 | Zubia et al. (1999) |
| Co. Vanguardia | Osvaldo Diez vein | Adularia | Ar/Ar | 153.4 ± 1.46, 152.9 ± 2.75, 155.1 ± 3.0 | Sharpe et al. (2002) |
| Manantial Espejo | Maria vein | Adularia | K/Ar | 124.8 ± 3.0, 142.6 ± 3.5 | Arribas et al. (1996) |
| Manantial Espejo | Maria vein | Adularia | | 134 ± 5 | Dube et al. (2000) |
| Manantial Espejo | Chon Aike Fm. | Zircon? | U/Pb | 159.9 ± 0.5 | Dube et al. (2000) |
| Martinetas | Coyote Vein | Adularia | | 167.9 ± 1.71 | Dube et al. (2000) |

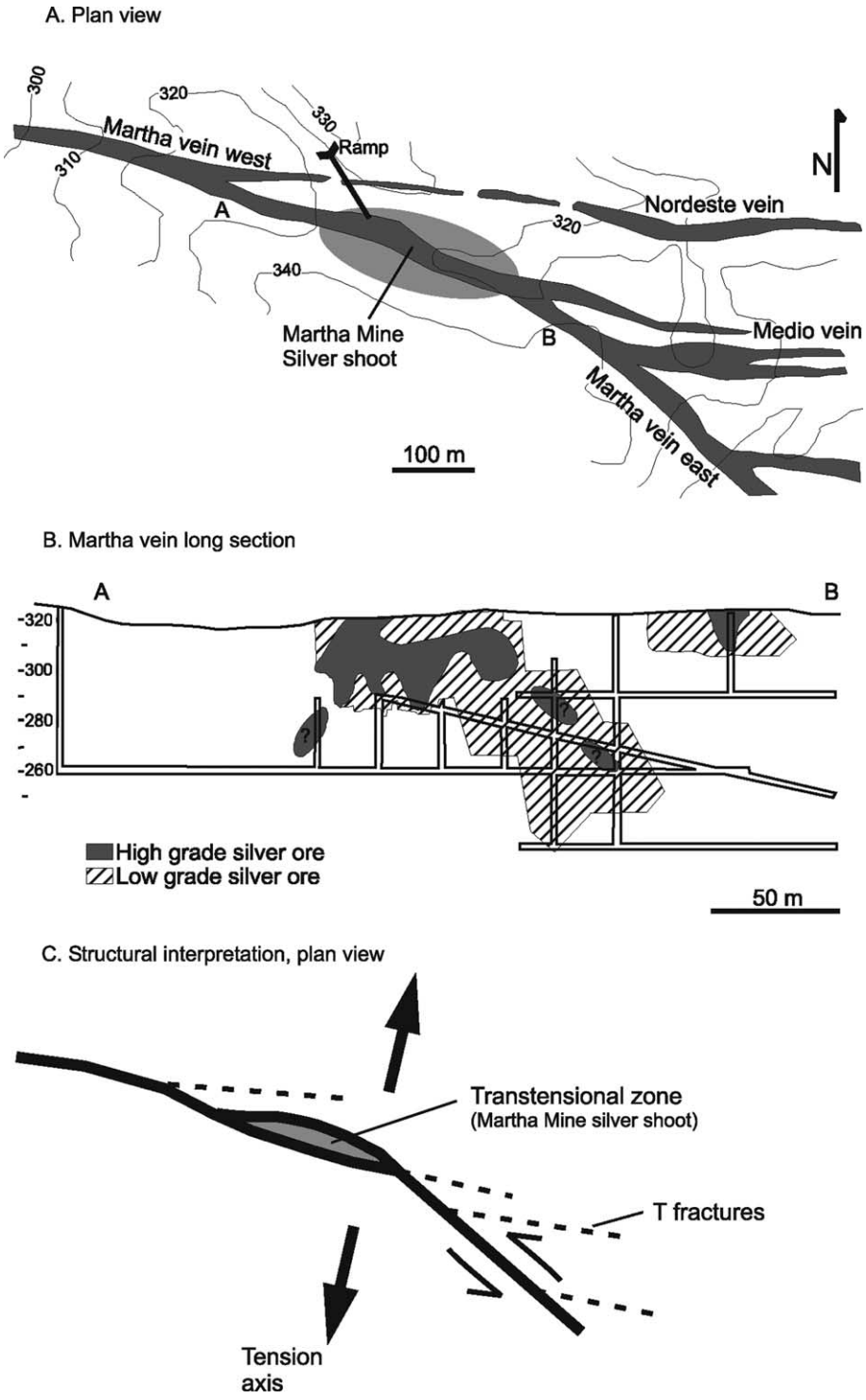


Fig. 6. Structural interpretation of the Martha vein, Bacon area. (A) Plan view of the Martha vein and associated extensional veins; topographic contours in meters. (B) Martha vein longitudinal section showing the location of the high-grade silver shoot. (C) Structural interpretation, the Martha Mine silver shoot develops in a structural opening related to a transtensional bend.

hosts high-grade ore (Fig. 6); its vein is hosted by a NW-trending left-lateral fault. A change in strike from southeast to east-southeast produced a jog that contains the high-grade silver ore.

The Ag/Au ratios in the Deseado Massif deposits and prospects vary (Table 2), showing an increase in silver content from the eastern Cerro Vanguardia to the western-most Martha mine. However, there are several exceptions to that pattern (e.g., La Josefina prospect), and more data are required for a more conclusive statement.

Only two deposits are, or have been, in production: Cerro Vanguardia and Martha mine. There are also several

Table 2
Gold and silver grades and salinity and temperature of homogenization of fluid inclusions in quartz for different deposits of the Deseado Massif

| Project | Au (g/t) | Ag (g/t) | Ag/Au | FI in quartz TH (°C) salinity (wt%) | |
|---|---|---|---|---|---|
| Co. Vanguardia | 12[a] | 66.11[a] | 5.5 | 210–320[b] | 1.5–3[b] |
| El Dorado-Monserrat | 6.2[c] | 152.75[c] | 24.64 | 180–280[d] | 1.5–5.6[d] (1.8) |
| Manantial Espejo | 2.87[e] | 191[e] | 66.55 | 200–320[e] | 0.35–6.5[e] |
| La Josefina | 2.4[f] | 18[f] | 7.5 | 200–280 [g] | 0.18–15 [g] |
| Bacon (Mina Martha) | 15.5[a] (in ore shoots) | 12000[a] | ~775 | | |
| Bajo Pobre | | | | 150–225[2] | |
| Manchuria | <7.44 [h] | <94.85 [h] | | 130–255 [h] | <3 [h] |

[a] Sunico, 2002.
[b] Schalamuk et al., 1999a.
[c] Echavarria and Etcheverry, 1998.
[d] This work.
[e] Schalamuk et al., 1999b.
[f] Fernández, pers. comm.
[g] Ríos, 2000.
[h] Tessone, 1999.

prospects at an advanced stage of development, such as San José and Manantial Espejo.

In the following sections, we focus on one Deseado Massif epithermal deposit, El Dorado-Monserrat, and use it to understand the geologic setting, ore controls, and paragenesis of the Deseado Massif epithermal deposits.

## 5. El Dorado-Monserrat

### 5.1. Local geology

The geology of the El Dorado-Monserrat area is characterized by andesite lavas of the Bajo Pobre Formation exposed in uplifted blocks and bounded by generally east-striking faults (Fig. 7). In general, these rocks are microporphyritic with abundant microphenocrysts of plagioclase, clinopyroxene (usually strongly altered and fractured with reaction rims of amphibole), and scarce smaller crystals of orthopyroxene. The matrix usually contains plagioclase, small crystals of orthopyroxene (hypersthene), and clinopyroxene (augite) that constitute a microlitic texture, with local changes to fluidal or intergranular texture.

In addition to lavas, volcanic breccias are present and composed of andesite and basalt clasts ranging in size from a few centimeters to almost 1 m across, with a dark gray, massive matrix. These volcanic breccias are genetically, spatially, and temporally linked to the andesites.

In the El Dorado-Monserrat area, Jurassic silicic volcanism was associated with a small caldera approximately 6 km in diameter, which is filled with several ignimbritic flows (Echavarría, 1999). These ignimbrites are mainly porphyritic rhyolites with many phenocrysts of quartz, K-feldspars (mainly sanidine), and biotite. Vitroclasts are abundant, as are lithoclasts of volcanic and acid pyroclastic rocks. A fine-grained, quartz-K-feldspar matrix, produced from devitrification, surrounds the different clasts. The tuffs interbedded in the ignimbrites, in general, are fine grained and vitreous and contain phenocrysts of quartz, scarce K-feldspar, and biotite. In the postcaldera stage, a monolithic collapse breccia, with clasts more than 2 m in diameter, formed along the borders of the caldera. The extra-caldera facies consists of finely stratified and reworked tuffs belonging to the La Matilde Formation. These rocks dip slightly outward from the margin of the caldera.

Finally, late volcanic activity resulted in the extrusion of acid volcanic domes along ring fractures located at the border of the caldera. These bodies are composed of pyroclastic rocks at the bottom, grade from thick lapillites to fine tuffs toward the top, and were capped by the effusion of viscous rhyolitic lavas.

The south and southwest portion of the area (Fig. 7) is covered by pyroclastic and reworked volcaniclastic rocks that constitute 100–200 m of subhorizontal stratified rocks. Uplift and tilting of horst blocks, such as the Cerro Rubio and Monserrat horsts (Figs. 7 and 8), occurred after Chon Aike deposition due to normal faulting. The rest of the area is covered by flows of intraplate alkaline basalts of Pleistocene age, which cover much of the area and thus obscure the interpretation of the preceding geologic events.

### 5.2. Mineralization

Two zones of low-sulfidation, epithermal Au–Ag mineralization have been recognized in the El Dorado-Monserrat area (Fig. 7). The El Dorado area is located approximately 6 km east of the El Dorado ranch and consists of discontinuous *en echelon* veins approximately 4500 m in total length. The veins were formed along an east-striking, right-lateral shear zone and are filled by massive, fine-grained quartz and massive or colloform chalcedony. Slight changes in color result from diffuse

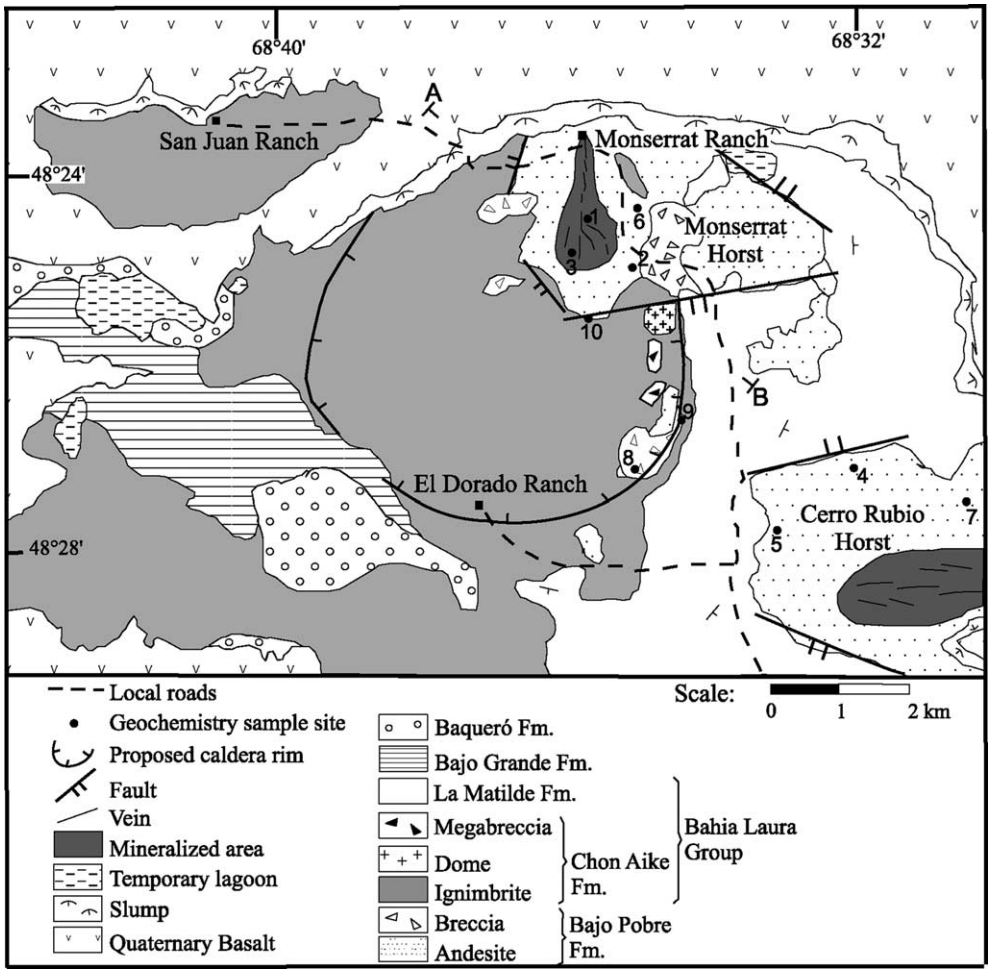


Fig. 7. Simplified geological map of El Dorado-Monserrat prospect. Location of Bajo Pobre Formation samples plotted in Fig. 10 are shown; cross-section in Fig. 8 corresponds approximately to line AB.

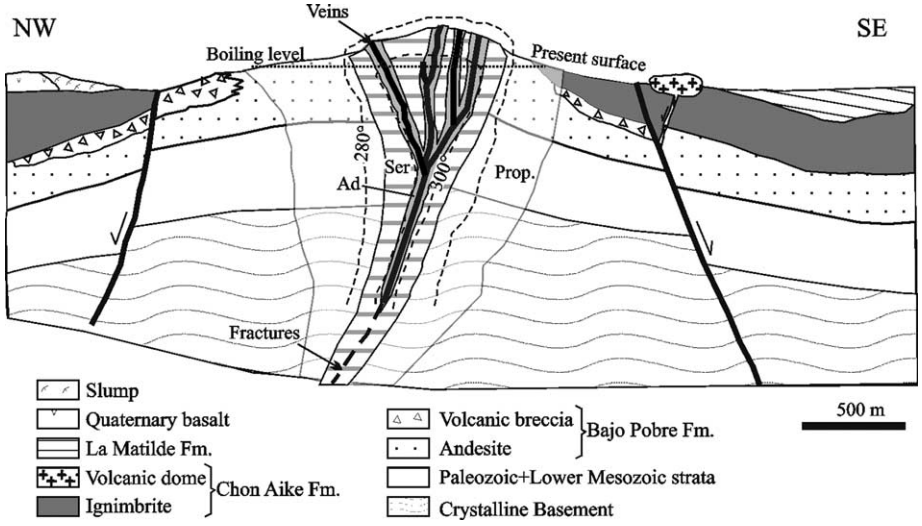


Fig. 8. Schematic cross-section of the Monserrat area showing the structural setting of the mineralization and distribution of hydrothermal alteration halos. The Monserrat horst corresponds to a fault-bounded horst block. The quartz-adularia alteration zone is closely related to mineralization; the propylitic zone is more widely distributed. Prop: propylitic alteration, Ser, sericitic alteration; and Ad, quartz-adularia alteration.

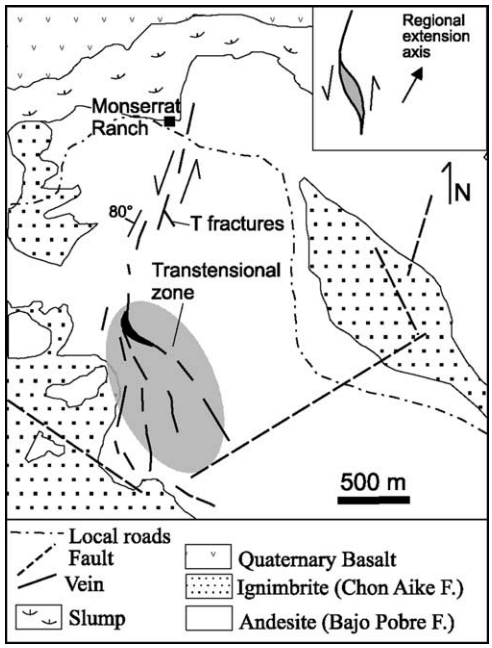


Fig. 9. Detailed plan view of the Monserrat veins. A bend in the left-lateral shear zone produces a transtensional area with the development of various veins. Inset shows regional structural interpretation.

banding. Isolated textures indicating quartz after carbonates are present. Samples from El Dorado contain low gold and silver, with an average of Au 0.09 ppm and Ag 14.5 ppm, and very low concentrations of base metals (<0.1%) (Echavarria and Etcheverry, 1998).

The second and most important mineralized area is located near the Monserrat ranch, approximately 4 km NW of the El Dorado veins. The total length of vein exposures is approximately 6 km, with an average thickness of 0.85 m, though there are large variations along-strike from 0.25 to 4 m. The veins occupy a north-striking, left-lateral shear zone. Continuous veins up to 3.5 m thick form in dilational jogs where the structure bends toward a SE-striking direction (Fig. 9).

Monserrat veins consist mainly of multistage quartz, with isolated breccias composed of hydrothermally altered wallrock and vein fragments cemented by fine-grained quartz. The average gold content of four sampled veins is 6.2 ppm, whereas silver reaches 153 ppm (Echavarria and Etcheverry, 1998). Base metals are present in very low concentrations (<0.15%), and neither base metal sulfides nor their weathering products have been observed in outcrop.

### 5.3. Hydrothermal alteration

On the basis of the mineral paragenesis and mineralogy, three types of hydrothermal alteration have been defined: quartz-adularia, sericitic, and propylitic (Fig. 8). The quartz-adularia zone is developed around quartz veins and ranges from a few centimeters to 1 m in thickness. It is characterized by quartz and adularia (based on the rhombic habit of the hydrothermal K-feldspar) that occur as fine veinlets replacing the fine-grained matrix of the volcanic rock and filling open spaces. The original texture and mineralogy of the volcanic rocks have been completely destroyed. Euhedral to anhedral adularia replaces most of the plagioclase (andesine) microphenocrysts; mafic minerals are totally replaced by a fine-grained intergrowth of quartz, pyrite, and abundant adularia, which is preferentially located toward the edge of the replaced crystal and usually constitutes up to 25% of its volume.

The quartz-adularia zone grades outward to an external halo of sericitic alteration up to 5 m wide. The sericitic alteration can be recognized by the bleaching of the andesitic wall rocks. Destruction of the wall rock texture and primary minerals is incomplete, so their original characteristics can still be recognized. Plagioclase microphenocrysts are altered to sericite (illite), and sericite is disseminated in the matrix of the volcanic rocks and/or fills open spaces.

Propylitic alteration, which represents the outermost hydrothermal alteration zone, occurs around the veins and quartz-adularia and sericitic zones. It forms a diffuse halo where the original texture of the host rocks has been preserved and is mainly restricted to phenocrysts. Plagioclase is slightly sericitized along fractures and cleavage planes, small calcite crystals are present in the core of some plagioclase grains, and the pyroxenes, the most abundant mafic mineral, are partially chloritized.

Whole-rock geochemical analyses were performed on fresh and hydrothermally altered andesite from the El Dorado-Monserrat area. Hydrothermal alteration produces a diagnostic pattern in the geochemical signature, with K- and Si-enrichment (Fig. 10), even hundreds of meters away from the veins.

Silicified fault-related ridges are widespread across the Deseado Massif; some are mistaken, or not easily differentiated from, the hydrothermal alteration related to mineralization. However, the geochemical signature of these ridges (Fig. 10) differs significantly from that of ore-related hydrothermal alteration. Both processes show Si-enrichment, whereas the silicified ridges lack the K-enrichment characteristic of ore-related hydrothermal activity.

### 5.4. Vein mineralogy

In order of decreasing abundance, vein mineralogy consists of quartz, barite, pyrite, adularia, magnetite, hematite, and electrum. Quartz and other silica minerals constitute more than 90% of the vein fill, whereas adularia + pyrite + Fe-bearing oxides + electrum form less than 5% of the rock within the ore zones. Silica minerals have been deposited in successive episodes, giving rise to a great variety of textures. Echavarría (1997b) describes these textures in detail and establishes their genetic significance and a chronological order for their formation. The textures

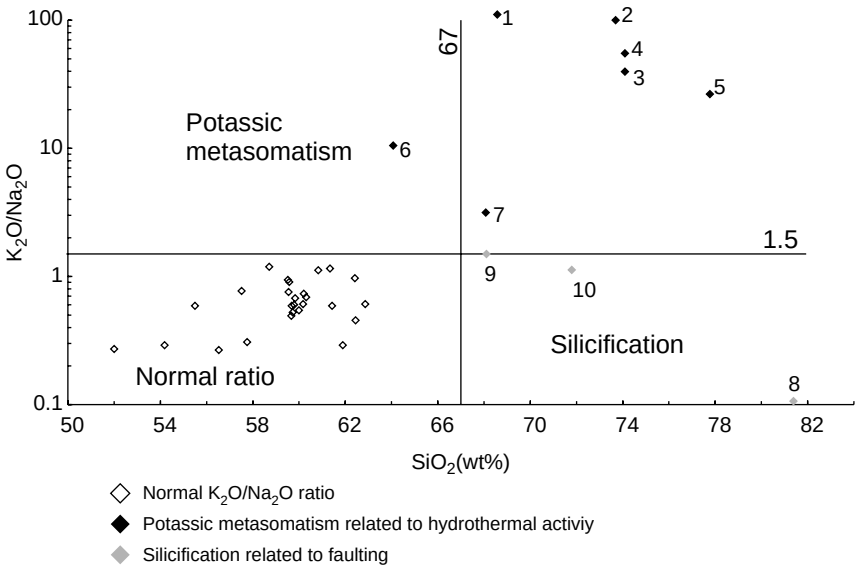


Fig. 10. $K_2O$ versus silica diagram for the Bajo Pobre Formation andesites of El Dorado-Monserrat. Samples related to hydrothermal alteration plot in the anomalous $K_2O$ and $SiO_2$ field; samples related to faulting display anomalous silica content but low $K_2O$. See Fig. 7 for the location of samples with anomalous K and/or Si content.

have been classified into three different groups based on their origin: (1) replacement quartz textures; (2) primary growth textures; and (3) recrystallization textures.

In replacement quartz textures, quartz completely replaces bladed calcite. Following Morrison et al. (1989), Dowling and Morrison (1990) and Dong et al. (1995), the replacement quartz textures identified at El Dorado-Monserrat are divided into four styles: (a) lattice bladed, which consists of intersecting quartz sheets with triangular spaces between them (Fig. 11(A)); (b) ghost bladed,

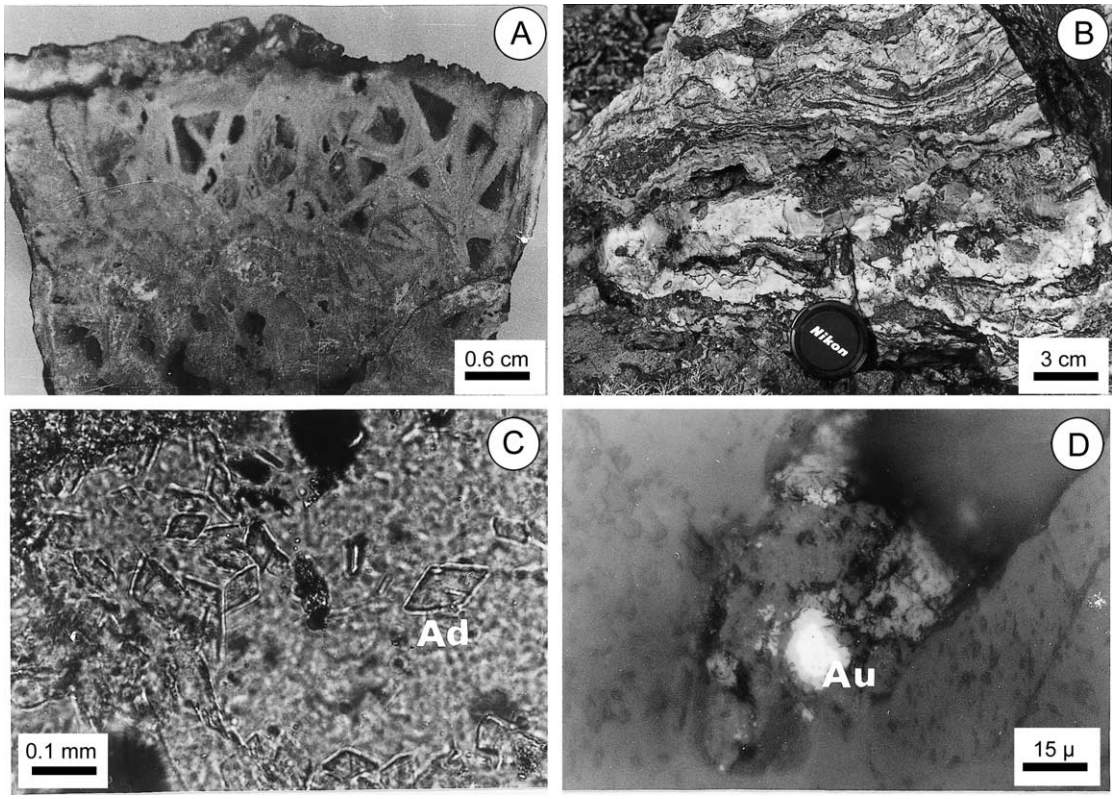


Fig. 11. (A) Lattice-bladed quartz texture: intersecting silica blades that form polyhedral cavities. (B) Crustiform texture, alternating with fine bands of microcrystalline quartz. (C) Euhedral adularia crystals with rhombic form (parallel polars). (D) Zoned gold grain with Ag-rich lighter sectors in the core.

in which the blades are differentiated from the matrix by outlines of impurities in thin section; (c) parallel; and (d) pseudo-acicular bladed, with substitution taking place preferably along laminae and forming very thin parallel or radiated sheets. In the Monserrat area, the calcite has been substituted by crystalline quartz with a subhedral to rectangular shape up to 1 mm in diameter, whereas at El Dorado, it is replaced by microcrystalline, milky quartz.

In primary growth textures, quartz fills open spaces as follows: (a) massive quartz textures, in which quartz occurs as subhedral crystals up to 1 mm in size, some of which are zoned with alternating milky and transparent bands and (b) crustiform–colloform textures, in which fine-grained quartz and chalcedony occur as successive, narrow bands (Fig. 11(B)) with alternating light colors (white, green, and pink).

Finally, recrystallization textures include (a) plumose or feathery texture, which features quartz crystals with feathered or splintery extinction; (b) mosaic texture that shows microcrystalline quartz of an average size of 8–20 μm, anhedral shape, and compact growth with interpenetrating grain boundaries; and (c) flamboyant texture, demonstrating radial extinction of the individual quartz-chalcedony crystals, though the whole grain has a circular external shape.

Barite, present as large, relatively pure crystals, forms veins less than 1 m thick and up to 300 m long that cut the quartz veins. Adularia is common in veins and veinlets. It forms subhedral to euhedral cuneiform crystals with rhombic sections up to 150 μm (Fig. 11(C)). According to electron microprobe analysis, the adularia composition is very close to the theoretical formula $KAlSi_3O_8$.

Pyrite is present as cubic euhedral crystals up to 5 mm in size and is associated with both the early precipitated adularia and the medium-grained quartz that were deposited during one of the last pulses. Magnetite and hematite are the principal primary iron-bearing minerals recognized in the deposit. Magnetite has been identified in restricted sectors, mainly in some veins of Monserrat as irregular crystals of less than 1 mm across and interspersed with adularia, quartz, and sericite. Hematite appears as both a space-filling mineral and an alteration product of magnetite. In the first case, hematite crystals have a tabular form, are up to 0.5 mm long, and show lamellar habits with red internal reflections and undulatory extinction. Where hematite is an alteration product of magnetite, crystals are smaller and develop along the octahedral cleavage of magnetite. Hematite has a very restricted distribution and is observed only in a few sectors of the Monserrat area.

Gold occurs as small, irregular grains up to 100 μm in diameter and is recognized only in massive quartz or quartz-filling bladed calcite cavities. Gold is yellow with lighter sectors in the center of the grains (Fig. 11(D)). Electron microprobe analyses (Table 3) show that the core of the grains consists of electrum with an average formula Au0.39–Ag0.58 and low contents of other elements (Table 3, points 1, 2, 6). Toward the borders, the silver content decreases significantly, and the gold reaches a high purity, around 98 wt% (Table 3, points 3, 4).

Although not directly observed, calcite was apparently a significant vein-forming mineral, as is evidenced by the quartz pseudomorphs of bladed calcite, up to 6 cm in length.

A paragenetic sequence can be interpreted from the vein mineralogy at El Dorado-Monserrat (Fig. 12). Early bladed calcite (as evidenced by quartz replacement textures) precipitated in open spaces from an ascending hydrothermal fluid, followed by adularia. Quartz precipitated in open spaces mainly with a massive texture; amorphous silica also was present according to the quartz recrystallization textures recognized. This quartz is associated with magnetite and pyrite and contains high-grade ore. Later, a fine crustiform-colloform band composed of chalcedony, fine-grained quartz, and pyrite was deposited with very low gold and silver contents (Echavarría and Etcheverry, 1998).

Table 3
Electron microprobe analyses for a zoned grain of gold from the Monserrat prospect. Points 1, 2, 5, and 6 are from the center of the grain, whereas points 3 and 4 are from the rim. Values expressed in wt%

| Elements | 1 | 2 | 3 | 4 | 5 | 6 |
|---|---|---|---|---|---|---|
| S | 0.06 | 0.019 | | 0.019 | 0.036 | 0.023 |
| Fe | 0.083 | 0.114 | 0.55 | 0.393 | 0.121 | 0.052 |
| Cu | 0.025 | | 0.053 | | 0.008 | 0.015 |
| Zn | 0.003 | | 0.015 | 0.03 | 0.026 | 0.047 |
| As | | 0.042 | | 0.028 | 0.019 | |
| Co | | | | | 0.006 | |
| Ni | | | | | | 0.008 |
| Bi | 0.542 | 0.35 | 0.062 | 0.582 | 0.219 | |
| Pb | 0.093 | | | | | 0.049 |
| Sb | | | | 0.019 | | |
| Ag | 43.6 | 45.61 | 0.368 | 0.348 | 25.16 | 45.32 |
| Cd | 0.621 | 0.529 | 0.017 | 0.072 | 0.487 | 0.621 |
| Te | 0.075 | 0.059 | | 0.012 | | 0.038 |
| Se | 0.559 | 0.603 | 0.909 | 0.928 | 0.867 | 0.694 |
| Au | 54.79 | 51.57 | 98.03 | 98.47 | 75.49 | 55.2 |
| Total | 100.4 | 98.9 | 100 | 100.9 | 102.4 | 102.1 |

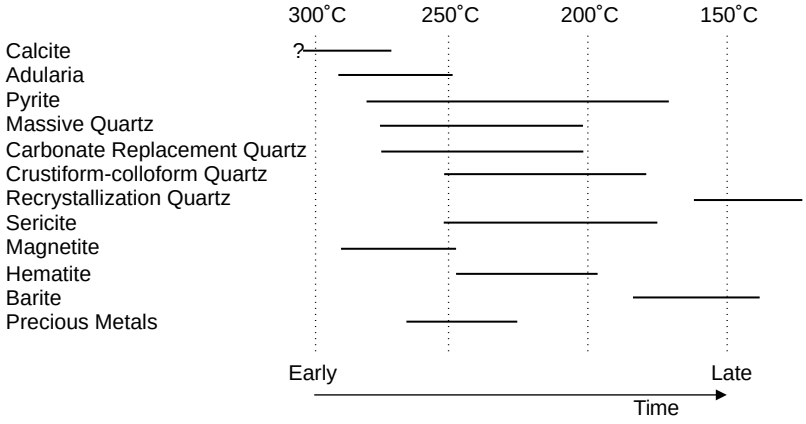


Fig. 12. Paragenetic sequence of mineralization at El Dorado-Monserrat; temperature range between 300 and 100 °C. This range was obtained from the fluid inclusion study in barite and massive and replacement quartz.

Then calcite became unstable and was completely replaced by quartz, thus developing the different replacement textures. Finally, in a post-ore stage, deposition of barite occurred in the form of thin veins, cross-cut by recrystallized quartz and chalcedony veinlets.

### 5.5. Fluid inclusions

#### 5.5.1. Quartz

Fluid inclusions (FI) were studied in quartz crystals with calcite replacement and massive textures. Quartz is euhedral to subhedral, with crystals up to 2 mm in diameter. Most inclusions are too small (<4 μm) to allow for a FI investigation. Secondary FI, aligned along fractures, are irregular in shape and size and contain a single liquid phase.

Primary FI are isolated or aligned along growth faces and reach up to 30 μm in size. The most common shapes are round and semirectangular. Primary FI are mostly two-phase, composed of liquid and vapor. The vapor/liquid ratio is variable, with the bubble occupying 10–50% of the inclusion. A few FI contain solids with irregular to rectangular shapes and a high birefringence. Because these solid phases are usually found in quartz with replacement texture, they could be small calcite remnants.

Microthermometric study of primary FI in six samples from the Monserrat area were carried out using a Chaixmeca −180°/600° freezing/heating stage mounted on a Leitz ortholux microscope. Ice melting temperatures ($T_m$) are between −0.5° and −3.5 °C (Fig. 13(A)). These values correspond to salinities between 0 and 5.6 wt% NaCl equiv., with a mode at 2.5 wt% NaCl equiv. The measured eutectic temperature ($T_e$) occurs between −20° and −22 °C, which corresponds to an $H_2O$–NaCl (−KCl) system with theoretical $T_e$ of −21.2 °C. The homogenization temperature ($T_h$) ranges between 160 and 280 °C, with a mode between 220 and 250 °C (Fig. 13(B)).

#### 5.5.2. Barite

Barite crystals from Monserrat samples contain a high concentration of FI, most of which are larger than 100 μm across. Primary inclusions are isolated and have a random distribution. Most are large, with a great proportion of single-phase liquid. Two-phase FI are composed of liquid and vapor, the latter occupying approximately 30% of the volume. The FI are rounded to irregular in shape, and some underwent total or partial necking.

Numerous planes of secondary FI cut the crystals in all directions. Two types of secondary FI are present: small FI are approximately 10 μm across, elongate, rounded, light

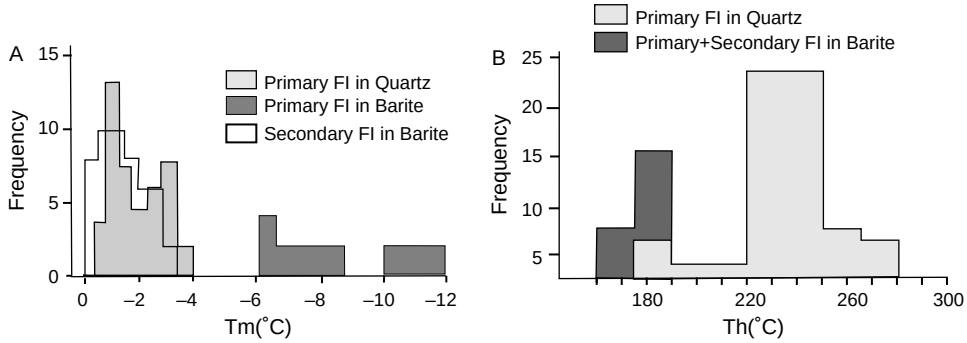


Fig. 13. Microthermometric measurements on fluid inclusions. (A) Ice melting temperatures in quartz and barite crystals. (B) Homogenization temperature for the same samples.

colored, and generally two phase, whereas larger FI are up to 80 μm across, elongated or semi-cubic with negative crystal shape, usually dark colored, and single phase (vapor).

The $T_m$ of primary FI occurs between −4 and 12 °C (Fig. 13(A)), corresponding to salinities between 6.4 and 16 wt% NaCl equiv. Homogenization temperatures range between 160 and 190 °C (Fig. 13(B)). In the case of secondary inclusions, $T_m$ ranges between 0 and −3.5 °C, corresponding to salinities between 0 and 5.6 wt% NaCl equivalent. The measured $T_e$ for this type of inclusions is −21.5 °C, corresponding to a $H_2O$–NaCl (–KCl) system. The $T_h$ values fall in the same range as those of the primary FI.

A Raman laser microprobe analysis study, performed at the Universidade Federal of Minas Gerais, Brazil, confirmed that FI in quartz and barite are an aqueous NaCl solution with insignificant quantities of noncondensable gases.

### 5.6. Stable isotopes

#### 5.6.1. Oxygen

Five samples of quartz with lattice- and ghost-bladed replacement textures, crustiform banding, and chalcedonic quartz were separated by hand picking and analyzed for oxygen isotopes by Actlabs, Canada.

The measured $\delta^{18}O$ values are between 6.1 and 8.6‰ (Table 4). For calculation of $\delta^{18}O$ of the fluid, a temperature of 250 °C was used for the samples with massive, calcite replacement and crustiform banding texture, whereas for the chalcedony, temperatures lower than 200 °C were assumed. Therefore, and using the equations by Matsuhisa et al. (1979) and Clayton et al. (1972), the $\delta^{18}O$ of the fluid in equilibrium with quartz was calculated to range between −1.9 and −3.1‰ (Table 4).

#### 5.6.2. Sulfur

$\delta^{34}S$ isotopic analyses were conducted on pyrite and barite. The $\delta^{34}S$ measured in pyrite intergrown with coarse-grained massive quartz is 0.8 ± 0.2‰, which at a temperature of 250 °C ($T_h$ of FI) corresponds to an $H_2S_{fluid}$ with $\delta^{34}S$ equal to −0.7‰, according to Ohmoto and Rye's (1979) equation. Barite is significantly enriched in $\delta^{34}S$; the four barite samples analyzed gave $\delta^{34}S$ values of 15.8–22.4‰.

Table 4
Oxygen isotopic composition of quartz. All samples are from the Monserrat area

| Sample | ($^{18}O_{Mineral}$ ‰ (meassured) | Temp.* (°C) | ($^{18}O_{fluid}$ ‰ (calculated) | Equation |
|---|---|---|---|---|
| DM20 | 6.2 | 250 °C | −2.7 | $1000\ln(=3.34(10^6/T^2)-3.31$ [1] |
| DM42 | 6.1 | 250 °C | −2.8 | $1000\ln(=3.34(10^6/T^2)-3.31$ |
| DM229 | 7 | 250 °C | −1.9 | $1000\ln(=3.34(10^6/T^2)-3.31$ |
| DM253 | 6.6 | 250 °C | −2.3 | $1000\ln(=3.34(10^6/T^2)-3.31$ |
| DM260 | 8.6 | 200 °C | −3.1 | $1000\ln(=3.38(10^6/T^2)-3.40$ [2] |

*Temperature used to calculate $\delta^{18}O_{fluid}$ value from $\delta^{18}O_{mineral}$ value. Matsuhisa et al. (1979) and Clayton et al. (1972) constants were used.

## 6. Discussion

### 6.1. Regional setting of the Deseado Massif epithermal mineralization

Major epithermal gold and silver deposits reveal a clear correspondence between the various epithermal types and specific volcanotectonic settings (John, 2001; Sillitoe, 2002a; Sillitoe and Hedenquist, 2003). Most typical low-sulfidation deposits are formed in a variety of continental and island-arc rifts characterized by bimodal volcanism (Sillitoe, 2002b) that may occur in intra-, near-, and backarc settings. In the case of the Deseado Massif, low-sulfidation epithermal mineralization is related to subaerial bimodal volcanism (Fig. 4) of a backarc-rift environment (Fig. 2), contemporaneous with rift tectonism (Figs. 2 and 3). Other examples of backarc settings for low-sulfidation epithermal deposits include those in the northern Great Basin of Nevada (e.g., Ivanhoe, Midas, Mule Canyon, Sleeper) associated with bimodal volcanic rocks of the northern Nevada rift, a product of backarc extension (John, 2001). Backarc rifting and bimodal volcanism during the Miocene in the Kitami region of northeastern Hokkaido, Japan, was also intimately related to the formation of many low-sulfidation veins (Watanabe, 1995). Finally, the Republic and Wenatchee low-sulfidation vein deposits of Eocene age in northern Washington formed in backarc grabens (Berger and Bonham, 1990).

A common characteristic of low-sulfidation deposits in bimodal rift settings is the relative abundance of bonanza gold shoots (Sillitoe, 2002a); almost 60% of all bonanza deposits occur in association with bimodal volcanism in rift settings (Sillitoe and Hedenquist, 2003).

Mineralization of the Deseado Massif is related to the final stages of the mostly rhyolitic Chon Aike volcanic cycle; the host rock can be either Chon Aike rhyolite or Bajo Pobre andesite. Although rhyolitic rocks are closely related to these deposits, the basaltic or intermediate component of the bimodal magmatic suites may play a fundamental role in the provision of sulfur, chloride, and even metals to the mineralizing hydrothermal fluids, as observed elsewhere (Noble et al., 1988; Hattori and Keith, 2001). Rhyolitic volcanic rocks normally lack any appreciable high-sulfidation mineralization (Sillitoe, 1993).

The epithermal vein deposits of the Deseado Massif are controlled by normal faults formed by extensional tectonism with the tension axis striking NNE. Fault systems striking ENE to EW are not favorable for ore deposition and result in discontinuous, thin veins with low gold and silver grades

(e.g., El Dorado). The fault systems that host the economic veins strike NNW to NW, and the veins are wide, continuous for several thousand meters, and have high gold and silver grades (Figs. 6 and 9; e.g., Cerro Vanguardia, Manantial Espejo, Martha Mine, San José, Monserrat). The ore shoots within the veins are related to dilational bends and jogs.

### 6.2. Temperature, salinity, and pH of hydrothermal fluids

The depth of formation of low-sulfidation epithermal deposits is usually shallow, within a few hundreds meters below surface (Hedenquist et al., 2000). Thus, the temperature corrections due to pressure are negligible, and the homogenization temperature of fluid inclusions can be considered similar to the trapping temperature (Bodnar et al., 1985). According to the FI study carried out at El Dorado-Monserrat, the main stage of the depositional process, which includes quartz, sericite, pyrite, and precious metals, took place at ~250 °C. However, the deposition of early minerals such as calcite and adularia probably started at higher temperatures than those for quartz deposition. Finally, late barite precipitation occurred between 190 and 160 °C. Based on the ice melting temperatures of primary inclusions in quartz, a representative salinity of the mineralizing hydrothermal fluids is 1.8 wt% NaCl equivalent. These results are similar to those found in other Deseado Massif epithermal deposits, such as Cerro Vanguardia, Manantial Espejo and La Josefina (Rios et al. in Schalamuk et al., 1999a; Ríos, 2000; Table 2).

The textural and mineralogical characteristics found at El Dorado-Monserrat suggest that boiling was the main process responsible for mineral deposition. Such characteristics include early bladed calcite precipitation, later replaced by quartz, and the presence of rhombic adularia. In epithermal environments, the precipitation of calcite in veins is most likely driven by the loss of $CO_2$ due to boiling (Henley et al., 1984). Furthermore, in many active geothermal systems, bladed calcite is commonly restricted to the boiling zone (Browne, 1978; Simmons and Christenson, 1994), though adularia is also closely related to boiling (Browne and Ellis, 1970). Evidence of boiling in FI at El Dorado-Monserrat is not clear, but in the Cerro Vanguardia, Manantial Espejo, and La Josefina districts, Rios et al. (in Schalamuk et al., 1999a) found evidence of boiling in FI in quartz. They also proposed that boiling was the main process responsible for mineral precipitation, including that of gold and silver.

The spatial distribution and time of formation of adularia and sericite help constrain the fluid chemistry and evolution. Adularia occurs inside and near the veins and formed during the first stages of mineral deposition. Sericite, however, has a widespread distribution and formed after the later stages of mineral deposition, which means that an important part of the fluids' evolution developed within the sericite stability field and reached only the requirements to form adularia in or near the veins where, probably due to boiling and $CO_2$ loss, the pH of the fluids increased. The absence of primary alunite and kaolinite indicates that the fluids never reached a pH acidic enough to form these minerals.

The $\delta^{18}O$ values calculated for the fluid are far from the composition of a magmatic fluid. These data, coupled with the low salinity of the mineralizing fluid, are more easily explained by a high proportion of meteoric waters. In contrast, taking into account the $\delta^{34}S$ value close to 0‰ found in pyrite, a magmatic source for the S, and probably the metals, cannot be ruled out. However, the assumption of a magmatic source for sulfides with $\delta^{34}S$ near 0‰ is a hazardous generalization when applied to hydrothermal environments and is valid only if we assume that the $H_2S$ concentration is equal to that of total sulfur in the system (Field and Fifarek, 1985).

## 7. Summary and conclusions

The Deseado Massif evolved during the Middle-Late Jurassic in a backarc extensional setting that favored the formation of widespread bimodal volcanism related to NNW-trending half-grabens. Numerous low-sulfidation epithermal vein systems were formed related to the final stages of this volcanism and hosted by either the Chon Aike or Bajo Pobre Formation. Veins are hosted by normal faults formed during a period of NNE extension, whereas the high-grade ore is located in ore shoots related to dilational bends and jogs.

El Dorado-Monserrat is a low-sulfidation epithermal deposit hosted by intermediate Jurassic volcanic flows of the Bajo Pobre Formation, in which the fracture zones striking NNW were the most favorable for fluid circulation and subsequent mineral deposition, with the formation of ore shoots related to dilational bends.

Mineralogical and textural evidence suggests that boiling was the main cause for hydrothermal mineral precipitation, including of gold and silver. Evidence for boiling includes the early generation of bladed calcite, later replaced by quartz, and the precipitation of adularia. Ore and gangue minerals of the ore stage precipitated from dilute fluids at temperatures between 225 and 275 °C. Post-ore barite precipitated during the final, waning stages of the hydrothermal system at temperatures below 190 °C.

On the basis of the geological and tectonic setting of the Deseado Massif and the characteristics of the ore deposits described, we conclude that the massif represents a geological environment with high potential for the exploration of low-sulfidation vein systems, mainly high-grade Au–Ag bonanza systems. However, significant high-sulfidation ore deposits are typically absent in this volcanic setting.

## Acknowledgements

This study is part of the 'Deseado Massif epithermal ore deposits' project sponsored by CONICET, Argentina. The support from the staff of the Mineral Resources Institute of La Plata University is gratefully acknowledged. Antonio Arribas and Agustin Martin Izard are sincerely thanked for reviewing early versions of the manuscript. We also thank Jeff Hedenquist, Eric Nelson, and Peter Cobbold for their reviews and constructive comments.

## References

Alric, V., Feraud, G., Bertrand, H., Haller, M., Labudia, C., Zubia, M., 1995. $^{40}Ar/^{39}Ar$ dating of patagonian jurassic vulcanism: new constraints on Gondwana break up, European union of geosciences, Strasburgo 1995 (Abstract).

Alric, V., Haller, M., Feraud, G., Bertrand, H., Zubia, M., 1996. Cronología $^{40}Ar/^{39}Ar$ del vulcanismo jurásico de la patagonia extraandina, XIII Congreso Geológico Argentino Actas, Tomo. Asociación Geológica Argentina, Buenos Aires pp. 243–250.

Archangelsky, S., 1967. Estudio de la formación baqueró. Cretácico inferior de Santa Cruz, Argentina. Revista del museo de la plata (nueva serie). Paleontología, 63–171.

Arribas Jr., A., Schalamuk, I.B., de Barrio, R.E., Fernández, R.R., Itaya, T., 1996. Edades radimétricas de mineralizaciones epitermales auríferas del Macizo del Deseado, provincia de Santa Cruz, Argentina. Actas XXXIX Congreso Brasilero de Geología, IGCP N° 342 'Age and isotopes of South American Ores' vol. VII. p. 254-257.

Berger, B.R., Bonham Jr.., H.F., 1990. Epithermal gold-silver deposits in the western united states: Time-space products of evolving plutonic, volcanic and tectonic environments. Journal of Geochemical Exploration 36, 103–142.

Bodnar, R.J., Reynolds, T.J., Kuehn, C.A., 1985. Fluid inclusion systematics in epithermal systems. Reviews in Economic Geology 2, 73–97.

Browne, P.R.L., 1978. Hydrothermal alteration in active geothermal fields. Annual Reviews in Earth and Planetary Sciences 6, 229–250.

Browne, P.R.L., Ellis, A.J., 1970. The ohaaki broadlands hydrothermal area, New Zealand: mineralogy and related geochemistry. American Journal of Science 269, 97–131.

Bruhn, R., Stern, Ch., De Wit, M., 1978. Field and geochemical data bearing on the development of a Mesozoic volcano-tectonic rift zone and back-arc basin in southermost South America. Earth and Planetary Science Letters 41, 32–46.

Cazaneuve, H., 1965. Datación de una toba de la Fm. Chon Aike (provincia de Santa Cruz), por el método potasio-argón. Ameghiniana, Revista de la Asociación Paleontológica Argentina IV (5), 156–158.

Chernicoff, C.J., Salani, F.M., 2002. Identificación de calderas asociadas a las volcanitas de la Formación Chon Aike en la región del Río Seco, provincial de Santa Cruz. In: XV Congreso Geológico Argentino, El Calafate, Tomo vol. II. Asociación Geológica Argentina, Buenos Aires, pp. 23–28.

Clayton, R.N., O'Neil, J.R., Mayeda, T., 1972. Oxygen isotope exchange between quartz and water. Journal of Geophysical Research 77, 3057–3067.

de Barrio, R.E., 1989. Aspectos geológicos y geoquómicos de la Formación Chon Aike (Grupo Bahóa Laura), en el noroeste de la provincia de Santa Cruz. Unpublished Ph. D. Thesis. UNLP, La Plata, Argentina.

de Barrio, R.E., 1993. El vulcanismo ácido jurásico en el noroeste de Santa Cruz, Argentina. Actas XII Congreso Geológico Argentino, Buenos Aires, Tomo vol. IV. pp. 189–198.

de Barrio, R.E., Panza, J.L., Nullo, F.E., 1999. Jurásico y Cretácico del Macizo del Deseado, provincia de Santa Cruz. In: Caminos, R. (Ed.), Geología Argentina, SEGEMAR. PP. 511–527 (Buenos Aires).

De Giusto, J.M., Di Persia, C., Pezzi, E., 1980. Nesocratón del Deseado Geología Regional Argentina II. Academia Nacional de Ciencias, Córdoba pp. 1389–1430.

Del Blanco, M., Echavarría, L., Echeveste, H., Etcheverry, R., Tessone, M., Mondelo, R., 1994. Estancia La Josefina, un nuevo prospecto aurífero en el Macizo del Deseado, Provincia de Santa Cruz, Argentina. Actas International Minning Meeting, Buenos Aires, pp. 93–99.

Del Blanco, M., Echavarría, L., Tessone, M., 1994b. Manifestaciones polimetálicas en la estancia La Sarita, Pcia. de Santa Cruz II Reunión de Mineralogía y Metalogénesis Actas, La Plata 1994 pp. 41–48.

Di Persia, C.A., 1960. Acerca del descubrimiento del Precámbrico en la Patagonia Extraandina (provincia de Santa Cruz) I Jornada Geológica Argentina Actas, Tomo II 1960 pp. 65–68.

Dong, G., Morrison, G.W., Jaireth, S., 1995. Quartz textures in epithermal veins in Queensland: Classification, origin and implication. Economic Geology 90, 1841–1856.

Dowling, K., Morrison, G.W., 1990. Application of quartz textures to the classification of gold deposits using North Queensland examples. Economic Geology Monograph 6, 242–355.

Dube, B., Zubia, M.A., Dunning, G., and Villeneuve, M., 2000. Estudio geocronológico de los campos filonianos de baja sulfuración hospedados en la Formación Chon Aike en el Macizo del Deseado, Patagonia, Argentina, SEGEMAR report, Buenos Aires.

Echavarría, L.E. 1995. Depósito Epitermal Cuarzo-Aurífero El Dorado-Monserrat, Prov. de Santa Cruz. In V Congreso Nacional de Geología Económica Acta, San Juan, Argentina, PP. 414–425.

Echavarría, L.E., 1997. Estudio Geológico-Minero del Area El Dorado-Monserrat, Departamento Magallanes, Prov. de Santa Cruz. Unpublished thesis. Facultad de Ciencias Naturales y Museo, Universidad de La Plata, Argentina.

Echavarría, L.E., 1997. Texturas de cuarzo del depósito epitermal El dorado-monserrat, provincia de Santa Cruz. Descripción e implicancias genéticas. Revista Asociación Geológica Argentina 52, 491–503.

Echavarría, L.E., 1999. Evolución geológica y su relación con la mineralización epitermal en el área El Dorado-Monserrat, Macizo del Deseado, Argentinaí. Stvdia Geologica Salmanticensia (España) 35, 21–39.

Echavarria, L.E., Etcheverry, R.O., 1998. Características geoquímicas de la mineralización epitermal El dorado-monserrat, provincia De Santa Cruz, Argentina. Revista Geológica de Chile 25, 69–84.

Echeveste, H, Echavarría, L., Tessone, M., 1995. Prospecto aurífero 'La Josefina', un sistema hidrotrmal tipo Hot Spring, Santa Cruz, Argentina. In V Congreso Nacional de Geología Económica Acta, San Juan, Argentina, pp. 414–425.

Echeveste, H., Fernández, R., Bellieni, G., Tessone, M., Llambias, E., Schalamuk, I., Piccirillo, E., De Min, A., 2001. Revista Asociación Geológica Argentina 56, 548–558.

Feraud, G., Alric, V., Fornari, M., Bertrand, H., Haller, M., 1999. $^{40}Ar/^{39}Ar$ dating of the jurassic volcanic province of Patagonia: Migrating magmatism related to Gondwana break-up and sbduction. Earth and Planetary Science Letters 172, 83–96.

Fernández, R., de Barrio, R., 1994. Mineralizaciones de oro y plata del macizo del Deseado, provincia de Santa Cruz, Argentina. Revista Comunicaciones, Universidad de Chile 45, 59–66.

Fernández, R.R Echeveste, H., Echavarría, L. and Schalamuk, I.B. 1996. Control volcánico y tectónico de la mineralización epitermal del área La Josefina, Macizo del Deseado, Santa Cruz, Argentina. In XIII Congreso Geológico Argentino Actas, Tomo III: pp. 41–54.

Field, C.W., Fifarek, R.H., 1985. Light stable isotope systematics in the epithermal environment. Reviews in Economic Geology 2, 99–128.

Genini, A., 1988. Cerro Vanguardia, provincia de Santa Cruz. Nuevo prospecto auroargentífero. In III Congreso Nacional de Geología Económica Actas, Tomo III, 97–110.

Gorring, M.L., Kay, S.M., Zeitler, P.K., Ramos, V.A., Rubiolo, D., Fernández, I., Panza, J.L., 1997. Neogene patagonian plateau lavas: Continental magmas associated with ridge collision at the chile triple junction. Tectonics 16, 1–17.

Guido, D., de Barrio, R., and Schalamuk, I.B. 1999. Sinter silíceo jurásico en estancia La Marciana, Macizo del Deseado, Santa Cruz. In XIV Congreso Geológico Argentino Actas, Salta. Tomo 2:. Asociación Geológica Argentina, Buenos Aires, pp. 341–44.

Guido, D., Delupi, R., Lopez, R., 2002. Manifestación aurífera asociada al complejo de domos La Emilia, sector noroccidental del Macizo del Deseado, Santa Cruz. In XV Congreso Geológico Argentino Actas, El Calafate, Tomo II: Asociación Geológica Argentina, Buenos Aires, pp. 290–293

Guido, D., Tessone, M., and de Barrio, R., 2002. Domo riolítico La Aragonesa: vinculación con manifestaciones metalíferas, sector central del Macizo del Deseado, Santa Cruz. In: XV Congreso Geológico Argentino Actas, El Calafate, Tomo II: Asociación Geológica Argentina, Buenos Aires, pp. 365–369

Gust, D.A., Biddle, K.T., Phelps, D.W., Uliana, M.A., 1985. Associated middle to late jurassic volcanism and extension in southern South America. Tectonophysics 116, 223–253.

Hattori, K.H., Keith, J.D., 2001. Contribution of Mafic Melts to Porphyry Copper Mineralization: Evidence from Mount Pinatubo, Philippines, and Bingham Canyon, Utah. Mineralium Deposita, USA pp. 799–806.

Hedenquist, J.W., Arribas, A., Gonzalez Urien, E., 2000. In: Hagemann, S.G., Brown, P.E. (Eds.), Exploration for Epithermal Gold Deposits Gold 2000, Reviews in Economic Geology pp. 245–277.

Henley, R.W., Truesdell, A.H., Barton, P.B., 1984. Fluid-mineral equilibria in hydrothermal systems. Reviews in Economic Geology 1, 267.

Homovc, J.F., Constantini, L.A., 2001. Hydrocarbon Exploration Potential Within Intraplate Shear-Related Depocenters Deseado and San Julián Basins, Southern Argentina. AAPG Bulletin 85 2001 pp. 1795–1815.

Irvine, N.T., Baragar, W.R.A., 1971. A guide to the chemical classification of the common volcanic rocks. Canadian Journal of Earth Sciences 8, 523–548.

John, D.A., 2001. Miocene and early pliocene epithermal gold-silver deposits in the northern great basin, Western United States: Characteristics, distribution, and relationship to magmatism. Economic Geology 96, 1827–1854.

Kay, S.M., Ramos, V.A., Mpodozis, C., Sruoga, P., 1989. Late paleozoic to jurassic silicic magmatism at the gondwana margin: Analogy to the middle proterozoic in North America? Geology 17, 324–338.

Le Bas, M.J., LeMaitre, R.W., Streckeisen, A., Zanettini, B., 1986. A chemical classification of volcanic rocks based on the total alkali-silica diagram. Journal of Petrology 27, 745–775.

Lesta, P.J., Ferello, R., 1972. In: Leanza, A.F. (Ed.), Región Extraandina de Chubut y Norte de Santa Cruz Geología Regional Argentina. Academia Nacional de Ciencias, Córdoba, pp. 601–654.

Matsuhisa, Y., Goldsmith, J.R., Clayton, R.N., 1979. Oxygen isotopic fractionation in the system quartz-albite-anorthite-water. Geochimica et Cocmochimica Acta 43, 1131–1140.

Morrison, G.W., Dong, G., Jaireth, S., 1989. Textural Zoning in Epithermal Quartz Veins in Queensland Field Guide. James Cook University of North Queensland, Townsville. P. 25 (AMIRA porject P247).

Nelson, E.P., Dalziel, I.W.D., Milnes, A.G., 1980. Structural geology of the cordillera darwin-collisional-style orogenesis in the southernmost Chilean Andes. Eclogae Geologicae Helvetiae 73, 727–751.

Noble, D.C., McCormack, J.K., McKee, E.H., Silberman, M.L., Wallace, A.B., 1988. Time of mineralization in the evolution of the McDermitt caldera complex, Nevada-Oregon, and the relation of middle miocene mineralization in the northern great basin to coeval regional basaltic magmatic activity. Economic Geology, 859–863.

Ohmoto, H., Rye, R.O., 1979. Isotopes of sulfur and carbon. In: Barnes, H.L. (Ed.), Geochemistry of hydrothermal ore deposits, second ed. Wiley, New York, pp. 509–567.

Pankhurst, R.J., Leat, P.T., Sruoga, P., Rapela, C.W., Marquez, M., Storey, B.C., Riley, T.R., 1998. The chon aike province of patagonia and related rocks in West Antarctica: a silicic large igneous province. Journal of Volcanology and Geothermal Research 81, 113–136.

Pankhurst, R.J., Rapela, C.W., 1995. Poduction of jurassic rhyolite by anatexis of the lower crust of patagonia. Earth and Planetary Science Letters 134, 23–36.

Pankhurst, R.J., Sruoga, P., Rapela, C., 1993. Estudio geocronológico Rb/Sr de los Complejos Chon Aike y El Quemado a los 47° 30′ L.S. In XII Congreso Geológico Argentino Actas, Mendoza, Tomo IV, pp. 171–178.

Panza, J.L., 1995. Descripción geológica de la Hoja 4969-II, Tres Cerros, prov. de Santa Cruz, Secretaría de Minería de La Nación. Boletín n° 213, Buenos Aires, Argentina 1995 p. 103.

Panza, J.L., Franchi, M.R., 2002. Magmatismo basaltico cenozoico extrandino. In: Haller, M.J. (Ed.), Geología y Recursos Naturales de Santa Cruz, Relatorio del XV Congreso Geológico Argentino. Asociación Geológica Argentina, Buenos Aires, pp. 201–236.

Panza, J.L., Haller, M.J., 2002. El volcanismo jurásico. In: Haller, M.J. (Ed.), Geología y Recursos Naturales de Santa Cruz, Relatorio del XV Congreso Geológico Argentino. Asociación Geológica Argentina, Buenos Aires, pp. 89–102.

Ramos, V., 2002. Evolución Tectónica. In: Haller, M.J. (Ed.), Recursos Naturales de Santa Cruz, Relatorio del XV Congreso Geológico Argentino. Asociación Geológica Argentina, Buenos Aires, pp. 365–387.

Reimer, W., Miller, H., Mehl, H., 1996. Mesozoic and Cenozoic palaeo-stress fields of the southern Patagonian Massif deduced from structural and remote sensing data. In: Storey, B.C., King, E.C., Livermore, R.A. (Eds.), Weddell Sea tectonics and Gondwana Break-up, vol. 108 Geological Society Special Publication, pp. 73–85.

Riccardi, A.C., 1983. The Jurassic of Argentina and Chile. In: Moullade, M., Nairn, A.E. (Eds.), The phanerozoic geology of the world II, the Mesozoic. Elsevier, Amsterdam, pp. 201–263.

Riley, T.R., Leat, P.T., Pankhurst, R.J., Harris, C., 2001. Origins of large volume rhyolitic volcanism in the Antarctica Peninsula and Patagonia by crustal melting. Journal of Petrology 42, 1043–1065.

Ríos, F.J., 2000. Fluid evolution in the La Josefina Au-epithermal system, Macizo del Deseado, Southern Patagonia, Santa Cruz, Argentina. Revista Brasileira de Geociencias 30, 769–774.

Sanders, G., 2000. Regional geologic setting of the gold-silver veins of the deseado massif, Southern Patagonia, Argentina. Argentina Mining 2000 Conference, Mendoza, Argentina 2000 p. 58.

Schalamuk, I.B., de Barrio, E.R., Zubia, M.A., Genini, A., Echeveste, H., 1999a. Provincia auroargentífera del deseado, Santa Cruz. In: Zappettini, E. (Ed.), Recursos Minerales de la República Argentina, SEGEMAR, pp. 1177–1188 (Buenos Aires).

Schalamuk, I.B., de Barrio, E.R., Zubia, M.A., Genini, A., 2002. Mineralizaciones auro-argentíferas del Macizo del Deseado y su enfoque metalogénico. In: Haller, M.J. (Ed.), Geología y Recursos Naturales de Santa Cruz, Relatorio del XV Congreso Geológico Argentino, pp. 679–713 (Buenos Aires).

Schalamuk, I.B. Etcheverry, R.O. and Echeveste, H. 1994. Consideraciones geológicas y metalogénicas del área comprendida entre los 69° 24′ a 69° 45′ de Longitud Oeste a los 48° 45′ a 48° 49′ de Latitud Sur, Prov. de Santa Cruz, Argentina. In: International Mining Meeting Acta, Buenos Aires, 87–92.

Schalamuk, I.B., Fernández, R.R., Etcheverry, R.O., 1995. Gold–silver epithermal veins in the Macizo del Deseado, Argentina. In: Pasava, J., Kribek, B., Zak, K. (Eds.), Proceedings of the third biennial SGA Meeting, pp. 385–388 (Praga).

Schalamuk, I.B., Zubia, M., Genini, A., Fernández, R.R., 1997. Jurassic epithermal Au–Ag deposits of patagonia Argentina. Ore Geology Reviews 12, 173–186.

Sharpe, R. Riveros, C, and Scavuzzo V. 2002. Stratigraphy of the Chon Aike Formation ignimbrite sequence in the Cerro Vanguardia Au–Ag

epithermal vein district. In XV Congreso Geológico Argentino Actas, El Calafate, Tomo II: Asociación Geológica Argentina, Buenos Aires, pp. 370–375

Sillitoe, R.H., 1993. Epithermal models: genetic types, geometrical controls and shallow features. Geological Association of Canada Special Paper 40, 403–417.

Sillitoe, R.H., 2002a. Rifting, bimodal volcanism, and bonanza gold veins. Society of Economic Geologists Newsletter48, 24–26.

Sillitoe, R.H., 2002b. Some metallogenic features of gold and copper deposits related to alkaline rocks and consequences for exploration. Mineralium Deposita 37, 4–13.

Sillitoe, R.H., Hedenquist, J.W., 2003. Linkages between volcanotectonic settings, ore-fluid compositions, and epithermal precious-metal deposits. In: Simmons, S.F., Graham, I. (Eds.), SEG Special Publication 10, pp. 315–343.

Simmons, S.F., Christenson, B.W., 1994. Origins of calcite in a boiling geothermal system. American Journal of Science 294, 361–400.

Spalletti, L., Iñiguez Rodríguez, M., Mazoni, M., 1982. Edades radimétricas de piroclastitas y vulcanitas del grupo bahía laura, gran bajo de san julián, Santa Cruz. Revista Asociación Geológica Argentina 37 (4), 483–485.

Sruoga, P., 1989. Estudio petrológico del Plateau Ignimbrítico jurásico a los 47° 30′ de latitud sur.Ph.D. Thesis. UNLP, La Plata, Argentina.

Sruoga, P., Irigoyen, M.V. 1987. Geología y descripción de los depósitos ignimbríticos jurásicos en el Gran Bajo de San Julián, provincia de Santa Cruz. In X Congreso Geológico Argentino Actas, Tucumán, Tomo 2, Asociación Geológica Argentina, Buenos Aires, pp. 51–54.

Sruoga, P., Palma, M.A., 1986. Los domos riolíticos jurásicos de los cerros laciar, moro, baguales y la pava, departamento de deseado, provincia de Santa Cruz. Revista Asociación Geológica Argentina 41, 397–401.

Sunico, E.A., 2002. La Mineria. In: Haller, M.J. (Ed.), Geología y Recursos Naturales de Santa Cruz, Relatorio del XV Congreso Geológico Argentino, pp. 665–677 (Buenos Aires).

Tessone, M., 1999. Mineralizaciones epitermales en el área de La Manchuria, Santa Cruz. In: Zappettini, E. (Ed.), Recursos Minerales de la República Argentina, SEGEMAR, pp. 1225–1230 (Buenos Aires).

Tessone, M., Del Banco, M., Macambira, M., Rolando, A.P., 1999. New radimetric ages of the chon aike and bajo pobre formations in he central zone of the deseado massif, Argentina. 2nd Simposio sudamericano de Geología Isotópica Actas, Córdoba 1999 pp. 132–135.

Uliana, M.A., Biddle, K.T., Cerdan, J., 1989. Mesozoic extension and the formation of Argentine Sedimentary Basins. In: Tankard, A.J., Balkwill, H.R. (Eds.), Extensional tectonics and stratigraphy of the North Atlantic margins, AAG Memoir, pp. 599–614.

Watanabe, Y., 1995. A tectonic model for epithermal au mineralization in NE hokkaido, Japan. Resource Geology Special 18, 257–269.

Zubia, M.A., Genini, A.D., Schalamuk, I.B., 1999. Yacimiento Cerro Vanguardia, Santa Cruz. In: Zappettini, E. (Ed.), Recursos Minerales de la República Argentina, SEGEMAR, pp. 1189–1202 (Buenos Aires).